

Experimental Examination on Forced Convection Heat Transfer in laterally Perforated finned Metal Matrix Composite Heat Sink



E. Nirmala devi, T.Rajesh

Abstract---Day by day a huge measure of research is proceeding to discover the cooling solutions for electronics including various applications for CPU, LED coolers, relay cooling frameworks. The serious issue including electronic parts cooling is the structure of heat sinks and their compatibility with the electronics for the predefined applications. Likewise, the quick-paced progressions in computing driving for the production of superior processors with incorporated complex circuits for which the cooling turned into a troublesome task which became challenging the existing market. This study targets building up a metal matrix composite (MMC) heat sink for low coefficient of thermal expansion (CTE) in electronic parts. Aluminum nitrate (AlN) takes like 12.5% (wt/wt) and mixed Aluminum (Al) to form metal matrix composite (MMC) prototype heat sinks. Prototype metal matrix composite (MMC) properties were evaluated experimentally. The modeling of the laterally perforated finned heat sink (LA-PFHS) is done Solid-works. The sinks are fabricated by using CNC machining. Two configurations of circular piercings on the fins are used in which the diameter and the spacing between piercings vary. In a rectangular insulated duct, the experimental analysis on the three metal matrix composite (MMC) heat sinks was performed under the phenomenon of forced convection at varying heat fluxes and at ambient conditions of temperature 30°C, pressure 101.326 KPa and 45% humidity. From 1.0 m/s to 4.0 m/s wind velocities and with an interval of 1 m/s the experimentation were carried out. Results show that the model III prototype metal matrix composite (MMC) heat sink proposed in this study shows a decrease in thermal resistance (R_{th}) by 50.51 %.

Keywords: forced Convection heat transfer, coefficient of thermal expansion, Metal Matrix Composites, heat sink, Reynolds number (R_e), Thermal resistance (R_{th}), Pressure drop, Pumping power.

I. INTRODUCTION

Thermal management has become very important challenging in today's electronics world. Overheating of electronic devices is a major issue in computing systems, avionics, battery management, and in different industrial and non-industrial applications. Electronic device life span can be increased by effective thermal management of the devices. Heat sink dissipates the heat from the electronic devices.

Revised Manuscript Received on May 30, 2020.

* Correspondence Author

E. Nirmala devi*, Associate Professor Department of Mechanical Engineering, Godavari Institute of Engineering and Technology, (Autonomous) Rajahmundry, India

T.Rajesh, PG Scholar Department of Mechanical Engineering, Godavari Institute of Engineering and Technology, (Autonomous) Rajahmundry, India

© The Authors. Published by Blue Eyes Intelligence Engineering and Sciences Publication (BEIESP). This is an open access article under the CC BY-NC-ND license (<http://creativecommons.org/licenses/by-nc-nd/4.0/>)

Air-cooled heat sinks have been commonly used as an answer for overseeing heat-related issues of electronics because of their adequacy, financial plausibility, unwavering quality, and straight forwardness in support. Air-cooled heat sinks are susceptible to relatively low heat transfer coefficients and have large base temperature variations.

Increasing air flow can overcome this problem but in real applications this method is limited as it increases the pumping capacity there by increasing the heat sink occupancy space. The surface boundary layer thickness dictates the heat transfer rates. Disruption of the laminar boundary layer to turbulent boundary layer increases the heat transfer from the surface. Boundary layer interruption uses the same phenomenon to enhance the heat transfer from the surface. Perforation of the fins is one among different boundary layer interruption techniques and lead to lighter systems that add weight advantage in the applications. Perforations can be made on the lateral surface or along the length. Shaeri et al. [1] investigated the pressure drop and heat transfer characteristics under different flow regimes. Square cross-sectional perforations along the lateral surface are used to perform an experimental investigation on the heat sink with flows varying from laminar to turbulent. Perforation size and porosity are taken to study thermo fluid characteristics of the heat sink. Compared to the solid fin heat sink, the mass-based thermal resistance (R_{th}) is lower by 41-51% for perforated heat sink under constant pumping power. Chingulpitak et al. [2] were proposed the thermal performance of plate-fin heat sink with lateral perforations. Circular cross-section perforations are made along the lateral surface. The effect of diameters and a different number of circular perforations on the fins of heat sinks are studied. The results showed that the 3 mm diameter and 75 perforations exhibited the 11.6 % more heat transfer rate than the solid fin heat sink. Kim et al. [3] had been numerically evaluated the performance of a rectangular perforations heat sink and branched fin heat sink. A new numerical volume averaging model is developed to study the performance of branched fin heat sink results showed that the branched fin heat sink and better thermal performance compared to the optimized rectangular fin heat sink. **Ahmed et al. [4]** numerically evaluated the effect of ribs inserted in the plate-fin heat sink. Position, height, and number are taken as the study parameters. Results showed 1.55 times increase in Nusselt number compared to the solid fin heat sink. **Cola et al. [5]** investigated the effect of carbon nano tubes as the interface materials for getting better thermal performance.

Experimental Examination on Forced Convection Heat Transfer in laterally Perforated finned Metal Matrix Composite Heat Sink

Environmental effects and standards of used electronic devices were laid out in the work. **Gwinn et al. [6]** investigated on thermal interface materials studied the effect of metallic oxide nano particles on the thermal performance of thermal grease compounds.

The results showed an increase in heat transfer rate compared to nonmetallic oxide thermal grease. **Kaczmar et al. [7]** researcher developed new methods to use liquid metals for the developing metal matrix composites using different casting techniques and various powder metallurgy processes. The economic feasibility of different manufacturing methods and their drawbacks are presented. Development of metal matrix composite (MMC) heat sinks with less change in density and enhancing thermal and mechanical properties is the focus of this work so that they can be used in low coefficient of thermal expansion (CTE) compatible avionic components. Stir casting is used to produce proposed combinations of the metal matrix composite (MMC) heat sinks. Thermal performance investigation is carried out at different flow regimes. **Shaeri et al. [8]** started his researcher on laterally perforated-finned heat sinks; from this he developed thermal performance. The air flow supposed to be laminar and non-bypass flows. Based on five porosities, he implemented with three different rectangular holes on the plate fin heat sinks LA-PFHSs. He put forward mass-based thermal resistance (R_{th}) as a performance indicator was calculated by multiplying the thermal resistance (R_{th}) and mass of the heat sink. The results showed that lateral perforated heat sinks with highest porosity at given perforation size provided thermal resistance (R_{th}) 45% lowers than conventional plate-fin heat sinks. In his research paper shows pressure drop at different Reynolds numbers (Re) with a change in porosities at a given perforation sizes. **Shaeri et al. [9]** numerical investigation in Perforations of a kind that small channels with square cross section are required ordered stream wise along the fin's length and their numbers mixed from 1 to 3. Numbers the action of mathematical calculations are proved with experimental research of the investigators and good concurrences were observed. Results show that the fins with longitudinal pores have worthy of attention heat transfer improvement in addition to the considerable downgrading in weight by estimates of the similarities with solid fins. **Al-Sallami et al. [10]** propound the heat transfer and pressure drop of the plate-fin heat sinks with an longitudinal notch, rectangular perforation and multiple circular perforations. They come to an end that notch and slot perforations result in good heat transfer and pressure drop compared to the circular perforations. **Shaeri et al. [11]** were studied of laterally perforated plate-fin heat sinks. The heat transfer and pressure drop of heat sinks were bestowed with different numbers and measurements of the rectangular perforation. **Dhanawade et al. [12,13]** presented an experimental investigation of studied on the heat transfer of the plate-fin heat sinks with lateral square perforations and circular perforations. Based on untested ideas studied was led by a guide under the conditions of turbulent and bypass flows. In that same perforation, the results demonstrated that the fin effectiveness of square perforated fin is better when compared to circular perforated fin. **Kim et al. [14-16]** presented an experimental investigation of studied on the

thermal performance of ordinary plate-fin heat sinks to find the optimum plate-fin thickness. **Wu et al. [17]** Researchers presented an experimental investigation has studied the integration of the volume of the heat sink as a restriction parameter. **Shaeri et al. [18]** presented an experimentally the numbers study of plate-fin heat sinks with rectangular perforations fin's along its length. The investigation of thermal performance heat sinks under the supposition of laminar and turbulence fluid flow and bypass flow. The comparison results indicated that the Nusselt number of the ordinary plate-fin heat sink was greater than that of the perforated plate-fin heat sink. **Jen et al. [19]** appreciable improvements founded by using longitudinal perforations; with a single perforation heat sink heat transfer rate is improved up to 80%. Likewise benefits have been described recently for strip fin heat sinks. **Subasi et al. [20]** experimental studied of aluminum (Al) heat sinks with hexagonal honeycomb fins. Finally he found out the optimal design parameters of the honeycomb fins in his experiment. The fin thickness, fin height, attack angle, and longitudinal pitch these are some variable parameters. In That advanced model was presented to obtain the optimum design parameters by considering at higher the Nusselt number at lower the friction factor.

II. EXPERIMENTAL SETUP

The experimental setup is illustrated in Fig. 1. Forced convection heat transfer treatment on the metal matrix composite (MMC) heat sink is maintained by placing in a closed duct under standard temperature and pressure (STP) conditions. A varying of heat flux (q) at 20W to 60 W was provided. The base temperature of 40°C is maintained throughout the experimental work before and after heat sink is measured by resistance temperature detector (RTD) inside the duct. The temperatures on the surface of the heat sink are measured using K-type thermocouples and Fluid flow velocity is measured by using hot-wire anemometer. A

Digital manometer is used to measure the pressure drop across the heat sink. For the visibility of the internal instrumentation, the setup is un-insulated on the top. The duct was made airtight. All the sides are insulated to prevent heat loss to the surroundings. Table.1 shows the different instruments used in the present work.

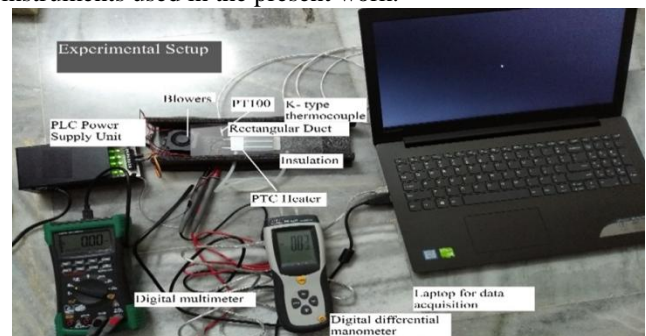


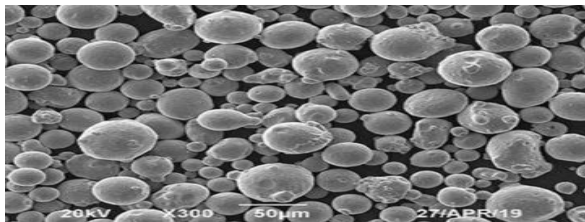
Fig 1. Experimental setup

TABLE 1. Specifications of Experimental setup

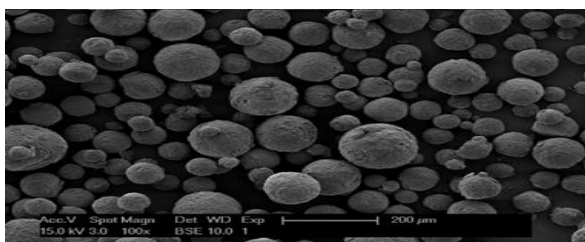
Instruments	Accuracy level	Use
PTC heater	± 1 W	Heating
RTD-PT100	± 0.1%	Temperature
Hotwire anemometer	± 0.1%	Wind velocity
K – type thermocouple	± 0.5%	Temperature
Digital multi meter	40ppm	Power
Duct(Area is 0.001125m ²)		Experiment
Blower	± 0.1%	Wind generator

III. PROPERTIES OF MATERIAL

Al micro-particles size ranging from 45-50 µm and AlN micro-particles size running 150-20 µm were utilized to prepare metal matrix composite (MMC) test specimens. In Fig 2(a) the scanning electron microscope (SEM) images for AL and in Fig 2(b) ALN micro- used in this study and were taken in the ratio of 87.5% Aluminum (Al) 12.5% Aluminum nitrate (AlN) properties are represented in Table 2.



(a)



(b)

Fig 2.Scanning electron microscope (SEM) of (a) Aluminum (Al) (b) Aluminum nitrate (AlN)

TABLE 2.Properties of Materials

Group	Density (gm/cm ³)	Young s Modulus (GPa)	coefficient of Thermal expansion (10 ⁻⁶ /°C)	Thermal Conductivity (W/m-K)	Specific Heat (J/g-K)
Aluminum (Al)	2.7	69	24	237	0.9
Aluminum nitrate (AlN)	2.762	94.07	21.063	254.621	0.879

A. Fabrication of metal matrix composite heat sink

The CAD model of a heat sink and to carry experimentation on the heat sink models with proposed

metal matrix composite (MMC) combination is illustrated in Fig 3.

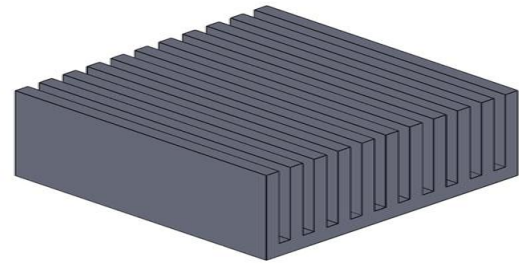


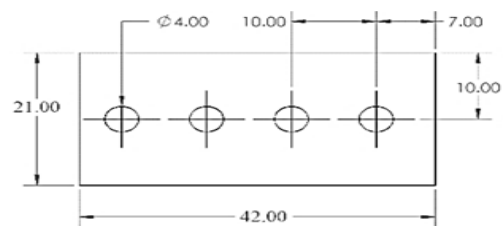
Fig 3.The CAD model of a Metal matrix composite (MMC) heat sink

For the designed models whose Lateral perforated-finned heat sink (LA-PFHS) which are represented in Fig. 4(a), 4(b) and 4(c), the codes such as G-codes and M-codes required for fabrication of the metal matrix composite (MMC) heat sinks prototypes by using CNC milling operations are developed using Solid works CNC package. On the 90 X 90 X 30 mm³ stir cast rectangular GI – metal matrix composite (MMC) bars the CNC milling operations are done to fabricate prototype metal matrix composite (MMC) heat sinks as per the designs carried out in Solid works. Fig. 4(a), 4(b) and 4(c) represent the lateral views and dimensions of the modeled heat sinks for the Sakkarin et al. [2], model II and model III.

Illustrates the CAD model of laterally perforated heat sink (LA-PFHS) with two rows of perforations in this study. Heat sinks were made of aluminum nitrate (AlN), and included 10 parallel channels (11 fins) with the fin thickness at 2.10 mm, and the channel length, height, and width at 42 mm, 17.9 mm, and 1.89 mm, respectively. The thickness of the heat sink base was at 3.10 mm. circular cross sectional perforations were fabricated on the lateral surfaces of the fins through the electrical discharge machining technique. Totally, 3 heat sinks were used in this study, which their geometrical parameters are summarized in Table 1. Experiments were performed using two perforation sizes at diameter 4 mm, thickness of the circular hole is 2.10 mm and hole to hole horizontal and vertical distance is 6 mm.

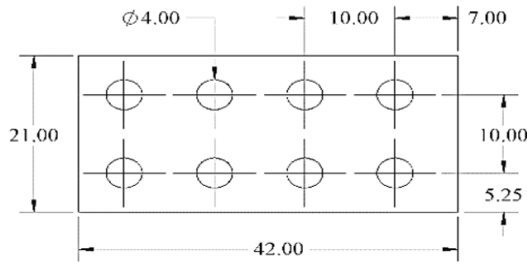


(a)



(b)

Experimental Examination on Forced Convection Heat Transfer in laterally Perforated finned Metal Matrix Composite Heat Sink



(c)

Fig 4. The lateral views dimensions of (a) Sakkari et al. [2] (b) Model II (c) Model III

TABLE 3. Geometrical information of the perforations associated with the different heat sinks in this present study

SI no.	Types of fins	Size of fin (l * b * h) mm	N o. of fins	Diameter of perforation (D) mm	Thickness of fin	Width of perforation (W) mm	No. perforations in each fin
1	Sakkari et al. [2]	42x42x 21	11	-----	2.1	-----	-----
2	With circular perforation (model -II)	42x42x 21	11	4	2.1	2.1	4
3	With circular perforation (model -III)	42x42x 21	11	4	2.1	2.1	8

B. Validation of experiments

Thermal resistance (R_{th}), heat transfer rate (Q), and Reynolds number (R_e) are the parameters used as performance evaluation indicators in the thermal evaluation of metal matrix composite (MMC) heat sink. The heat transfer rate from metal matrix composite (MMC) heat sink to surrounding air (Q) is given by

$$Q = m \cdot C_{pf} (T_{f out} - T_{f in}) \quad 1$$

Where C_{pf} is air specific heat, m is air mass flow rate, $T_{f in}$ and $T_{f out}$ are average temperatures at inlet and outlet respectively. The metal matrix composite (MMC) heat sink thermal resistance (R_{th}) is determined by

$$R_e = \frac{(T_{B,avg.} - T_{f,avg.})}{Q} \quad 2$$

Where the heat sink base temperature is given by $T_{B,avg.}$ and $T_{f,avg.}$ represents average air temperature. The Reynolds number (R_e) is given as

$$R_e = \frac{V_f D_i}{\nu} \quad 3$$

Where the velocity of air inside the channel is given V_f , ν represents kinematic viscosity and hydraulic diameter D_i is calculated by

$$D_i = \frac{4A_c}{P_c} \quad 4$$

Where P_c is represents perimeter of the flow channel and cross-sectional area of the channel is A_c .

The pumping power (P_m) is calculated from the total volumetric flow rate in the heat sink and the pressure drop (ΔP) is measured using differential manometer.

$$P_m = q_c \Delta P \quad 5$$

C. CFD Governing Equations

- Mass Conservation Equation (Equation of continuity):

$$\frac{\partial \rho}{\partial T} + \nabla \cdot (\rho \vec{v}) = 0 \quad 6$$

Where ρ = density and v = velocity of the fluid.

- Momentum Conservation Equation:

$$\rho \left[\frac{\partial \vec{v}}{\partial T} + (\vec{v} \cdot \nabla) \vec{v} \right] = f \quad 7$$

Where f = external force/ unit volume and f acts on the material volume.

- Energy Conservation Equation:

$$\frac{\partial}{\partial T} (\rho e) + \nabla \cdot [\rho \vec{v} e] = -\nabla \cdot (\sum_j h_i J_j) + S_h \quad 8$$

IV. RESULTS

To evaluate the signification of the forced convection heat transfer in the present experimental work. The Reynolds number (R_e) is the ratio of inertia force to viscous force, is the calculated for individual heat sinks. Although all the heat sinks were tested at the same input blower voltages, different wind velocity in the heat sinks resulted in various mass flow rates and in turn, a different range of Reynolds numbers (R_e), as observed in Fig 5. It can be seen that the mass flow rate of air inside the rectangular duct section increases gradually as the wind velocity changes from 1 m/s to 4 m/s.



The mass flow rate of air inside the rectangular duct shows turbulence characteristics as the Reynolds number (R_e) varies from 2055.5 to 8222 during experimentation.

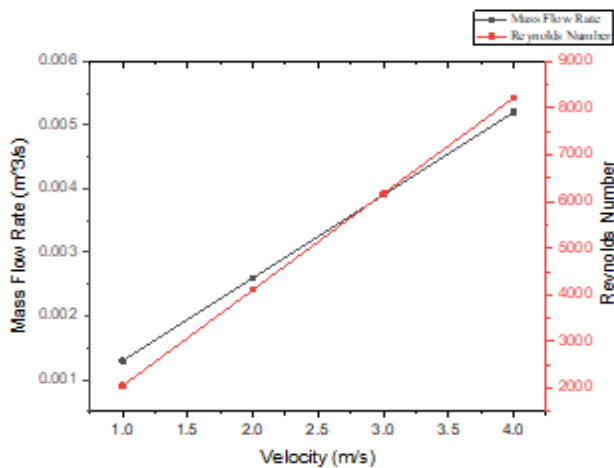


Fig5. Variation of Reynolds number (R_e) and mass flow rate with respect to wind velocity

Heat sink thermal resistances (R_{th}) due to changes in the Reynolds number (R_e) at a given perforation size are illustrated in Fig 6. Generally, LA-PFHSs are promising cooling devices to reduce thermal resistances (R_{th}) at a given Reynolds number (R_e). However, for designing such efficient metal matrix composite (MMC) heat sinks a detailed understanding of the roles of key geometrical parameters. It can be seen that the Sakkarin et al. [2] heat sink highest thermal resistance (R_{th}) of 6.3289 K/W at Reynolds number (R_e) is equal to 2055.5. Whereas at Reynolds number (R_e) equal to 2055 the thermal resistance (R_{th}) by model II is equal to 2.1765K/W and by the model III is equal to 1.2871K/W. The least thermal resistance (R_{th}) by the model III at Reynolds number (R_e) equal to 8222 which is equal to 0.1789K/W. Whereas at Reynolds number (R_e) equal to 8222 the thermal resistance (R_{th}) by model II is equal to 0.1960K/W and by the model having Sakkarin et al.[2] is 1.2871K/W.

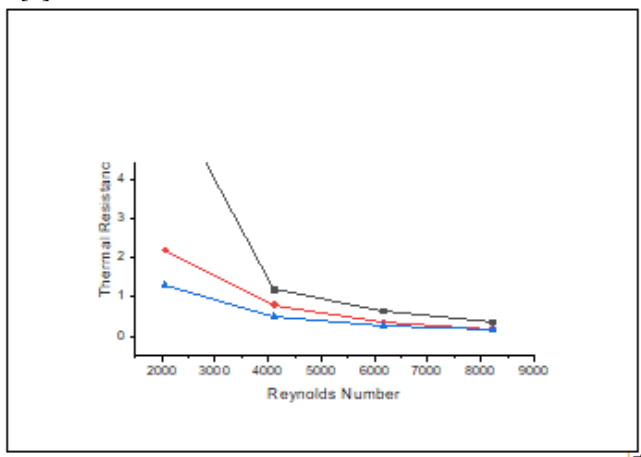


Fig 6. Thermal resistance (R_{th}) – Reynolds number (R_e)

The pressure drop founded by using differential manometer against Reynolds number (R_e) in the experimental analysis for the proposed prototypes of metal matrix composite (MMC) heat sink are plotted in Fig.

7. Despite the drawback of increased pressure drops by Lateral perforated-finned heat sink (LA-PFHS), these cooling systems experience a higher range of Reynolds numbers (R_e). This indicates that by Lateral perforated-finned heat sink (LA-PFHS) is potentially promising cooling devices gradually increase in pressure drop with respect to increase in Reynolds number (R_e) can be observed for the prototype metal matrix composite (MMC) heat sink models. The Sakkarin et al.[2] heat sink the highest pressure drop of 941Pa at Reynolds number (R_e) equal to 8222. Whereas at Reynolds number (R_e) equal to 8222 the pressure drop exhibited by model II is equal to 909 Pa and by the model III is equal to 897 Pa. Due to the lateral piercings, the pressure drops reduced for model II and model III heat sink prototypes.

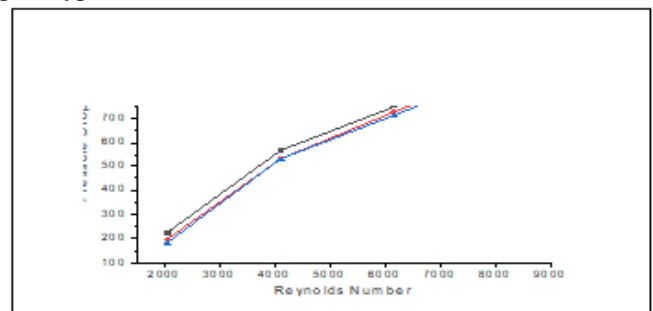


Fig 7. Pressure drop - Reynolds number (R_e)

The pumping power is the power required to drive the flow across the heat sink, and is one of the key parameters for designing an active cooling system, as such an increase in the pumping power may hinder using the cooling device regardless of its improved thermal performances. Therefore, in order to provide a practical insight about the advantages of thermal performances of Lateral perforated-finned heat sink (LA-PFHS)s are presented as functions of pumping powers instead of Reynolds numbers (R_e) throughout the study. The pumping power for the three models considered in the study is calculated using equation (5) and were plotted against Reynolds number (R_e) in Fig. 8. The pumping power increases gradually as the pressure drop increases with respect to increase in Reynolds number (R_e) for the metal matrix composite (MMC) heat sink models. At Reynolds number (R_e) equal to 2055.5 the pumping power values for the Sakkarin et al.[2] Model, Model II and model III are 0.2475 W, 0.2156 W, and 0.2013 W whereas at Reynolds number (R_e) equal to 8222 the pumping power values are 4.0463W, 3.9087W, and 3.8571W.

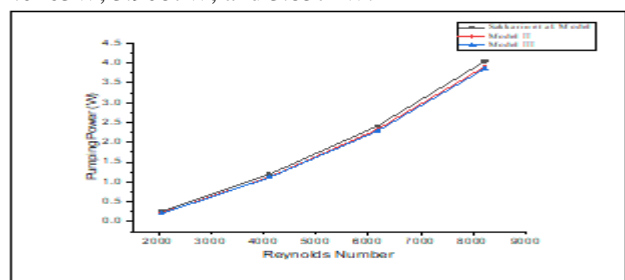
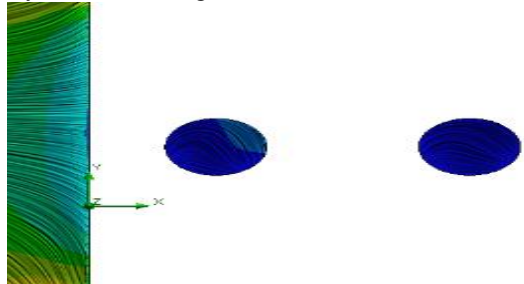


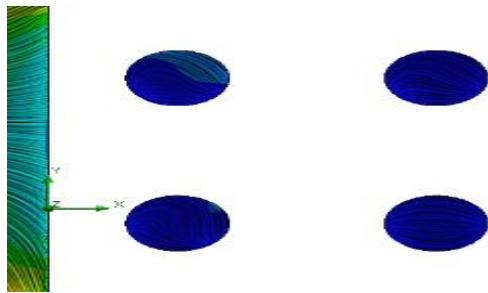
Fig 8. Pumping power- Reynolds number (R_e)

V. FLOW BEHAVIOR

The air flow behavior inside Lateral perforated-finned heat sink (LA-PFHS) is demonstrated with velocity vector. From the simulation results, the flow visualizations are presented in fig 9. As we can see, the flow impinging to the heat sink creates one vortex which occurs because of the jet impingement with the heat sink base. Relatively higher velocity results in a larger vortex for the heat sink.

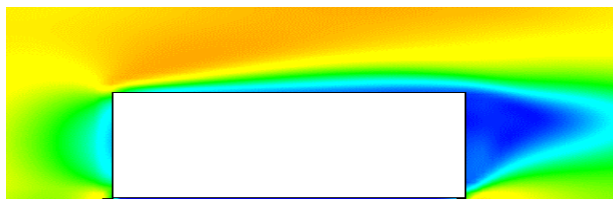


(a)

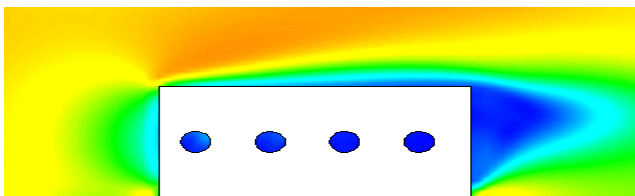


(b)

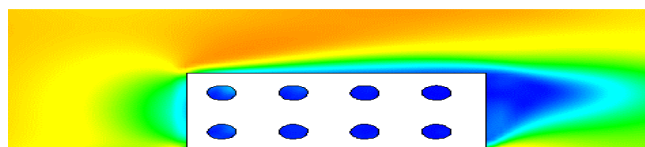
Fig 9. Flow recirculation in the lateral perforations for (a) Model II (b) Model III



(a)



(b)



(c)

Fig 10. Velocity contour for (a) sakkarin et al. [2] (b) Model II (c) Model III

D. Aluminum heat sink VS aluminum nitrate heat sink

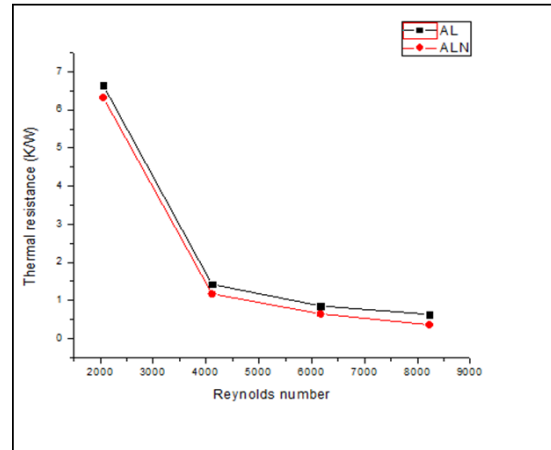


Fig.11 Thermal resistance (R_{th}) vs. Reynolds number (Re) (Al and ALN Solid fin heat sinks)

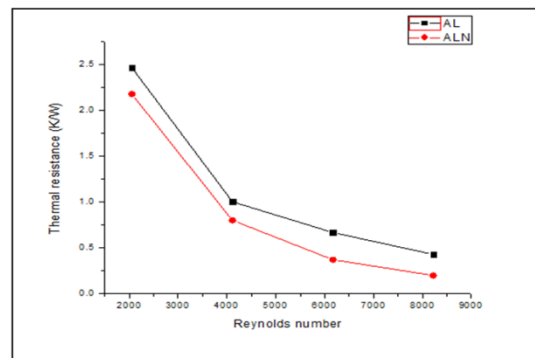


Fig.12 Thermal resistance (R_{th}) vs Reynolds number (Re) (Al and ALN Less perforations fin heat sinks)

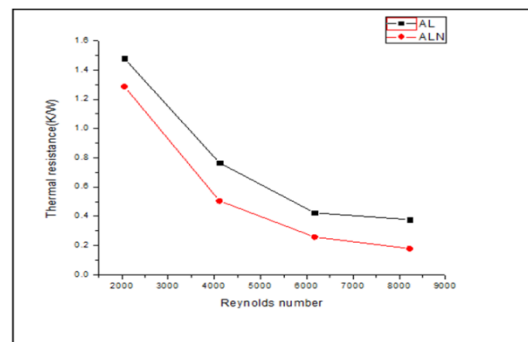


Fig.13 Thermal resistance (R_{th}) vs Reynolds number (Re) (Al and ALN More perforations fin heat sinks)

Fig.11, Fig.12 and Fig.13 shows that the Aluminum (Al) heat sink and aluminum nitrate (ALN) heat sink thermal resistance (R_{th}) variations with respect to Reynolds number (Re). Fig. 11 The aluminum nitrate solid fin heat sink thermal resistance (R_{th}) is 0.3615 (K/W) less than the aluminum solid fin heat sink thermal resistance (R_{th}) is 0.6327 (K/W) at maximum Reynolds number (Re) 8222. Similarly Fig.12 aluminum nitrate (ALN) heat sink thermal resistance (R_{th}) is 0.196 (K/W) less than Aluminum (Al) heat sink thermal resistance (R_{th}) is 0.4256 (K/W) at maximum Reynolds number (Re) 8222 and third Fig.

13 shows aluminum nitrate (AIN) heat sink thermal resistance is 0.1789 (K/W) less than Aluminum (Al) heat sink thermal resistance is 0.3772 (K/W) at maximum Reynolds number(R_e) 8222. In this three graphs Reynolds number (R_{th}) varied approximately and thermal resistance (R_{th}) decrease in the heat sink while thermal conductivity is increase.

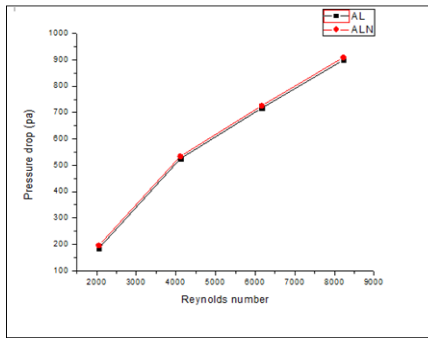


Fig.14 Pressure drops vs. Reynolds number (R_e) (Al and AIN Solid fin heat sinks)

heat sink Pressure drop is 899 P_a at maximum Reynolds number(R_e) 8222. and as shown in Fig.16 more perforations heat sink Pressure drop is 897 P_a aluminum nitrate (AIN) heat sink greater than aluminum(Al) heat sink Pressure drop is 882 P_a at maximum Reynolds number(R_e) 8222. In this three models Reynolds number very small variations accured on aluminum nitrate (AIN) and aluminum (Al) less perforations fin heat sinks.

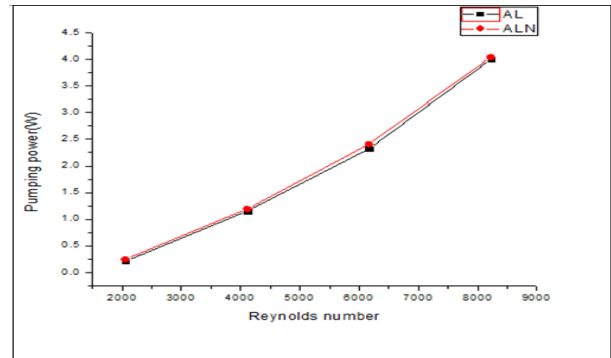


Fig.17 Pressure drops vs. Reynolds number (R_e) (Al and AIN Solid fin heat sinks)

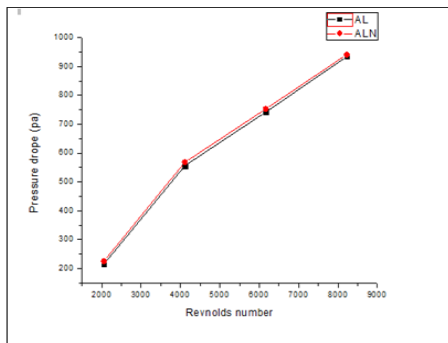


Fig.15 Pressure drops vs. Reynolds number (R_e) (Al and AIN Less perforations fin heat sinks)

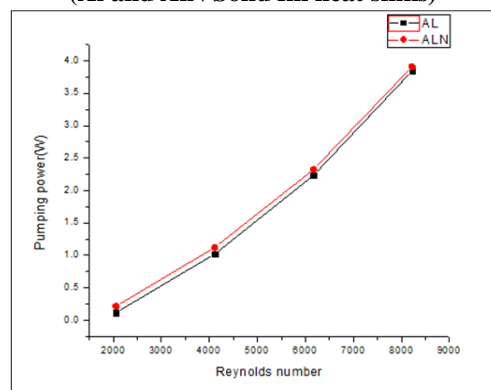


Fig.18 Pressure drops vs. Reynolds number (R_e) (Al and AIN Less perforations fin heat sinks)

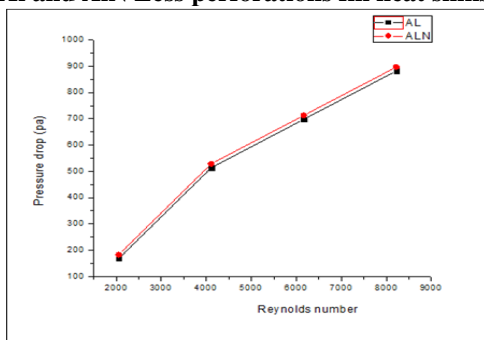


Fig.16 Pressure drops vs. Reynolds number (R_e) (Al and AIN More perforations fin heat sinks)

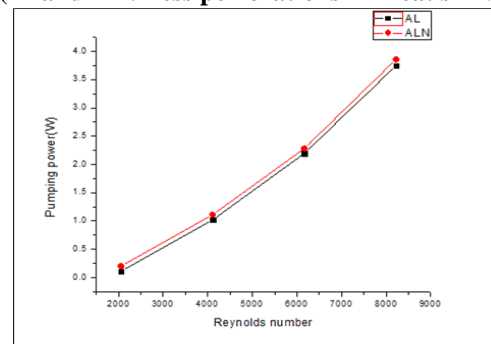


Fig.19 Pressure drops vs. Reynolds number (R_e) (Al and AIN More perforations fin heat sinks)

As shown in Fig.14, Fig.15 and Fig.16 the relationship between the pressure drop and Reynolds number (R_e) are investigated with aluminum (Al) and aluminum nitrate (AIN) heat sinks. Based on three graphs pressure drop variations in the laterally finned heat sinks as shown in Fig.14 the aluminum nitrate (AIN) solid fin heat sink Pressure drop is 941 P_a greater than aluminum (Al) solid fin heat sink Pressure drop is 934 P_a at maximum Reynolds number(R_e) 8222. similarly Fig.15 shows Less perforations fin heat sink aluminum nitrate (AIN) heat sink value is 909 P_a greater than aluminum (Al) Less perforations fin

As shown in above Fig.17, Fig.18 and Fig.19. variation of pumping power with respect to Reynolds number experimentally investigated with aluminum (Al) and aluminum nitrate (AIN) heat sinks. Pumping power variation depends on velocity of flows and as shown in Fig.17 pressure drop values consider solid fin heat sink aluminum nitrates (AIN) heat sink pumping power is 4.0463 W greater than aluminum (Al) heat sink Pumping power is 4.0001W at maximum Reynolds number(R_e) 8222.

Experimental Examination on Forced Convection Heat Transfer in laterally Perforated finned Metal Matrix Composite Heat Sink

similarly shown in Fig.18 Less perforations fin heat sinks aluminum nitrates (AlN) heat sink pumping power is 3.9087 W greater than aluminum (Al) heat sink pumping power is 3.8425W at maximum Reynolds number (R_e) 8222 and Finally shown in Fig.19 More perforations fin heat sinks aluminum nitrates (AlN) heat sink pumping power is 3.8571W greater than aluminum (Al) heat sink pumping power is 3.7444W at maximum Reynolds number (R_e) 8222. The three models maintain is velocities 0.0043 m³/s at maximum Reynolds number 8222. The aluminum nitrates (AlN) and aluminum (Al) heat sink flow velocities is same.

VI. CONCLUSION

Under turbulent flow regimes and at forced convection heat transfer characteristics of stir cast metal matrix composite (MMC) prototype heat sinks prepared by CNC machining were evaluated experimentally at Reynolds number (R_e) ranging from 2055.5 to 8222. Model III heat sink prototype showed improved thermal characteristics than model II and the heat sink model having Sakkarin et al.[2]. The thermal and mechanical properties of metal matrix composite (MMC) were density is increased 2.296% and the young's modulus increased 36.5 % from which it can be observed that unlike Aluminum (Al).The metal matrix composite (MMC) stir cast easily manufactured by simple techniques. The coefficient of thermal expansion (CTE) of metal matrix composite (MMC) reduced 8.4% and specific heat 1.897% less than Aluminum (Al) respective properties. Finally, the thermal conductivity is enhanced by 11.74% for metal matrix composite (MMC) than Aluminum (Al).This increment in thermal conductivity (K) and pressure drop-in coefficient of thermal expansion (CTE) and make it compactable for low coefficient of thermal expansion (CTE) for electronic parts cooling. The model III prototype metal matrix composite (MMC) heat sink proposed in this study shows a decrease in thermal resistance (R_{th}) by 50.51 % compared to the heat sink model having Sakkarin et al.[2].The flow recirculation caused the increase in heat transfer rate and a decrease in thermal resistance (R_{th}) for the model II and model III. For heat sinks, thermal resistance (R_{th}) reduction leads to enhancement in the heat transfer. Correspondingly, the heat sink's efficiency and effectiveness will also increase. From this study, it can be evaluated through the combination of Aluminum (Al) with Aluminum nitrate (AlN) increases density of the resultant metal matrix composite (MMC) the lateral piercings helps to maintain the weight of the designed heat sinks for respective applications and will be promising and compactable with low coefficient of thermal expansion (CTE) electronic and avionic instruments and the heat sinks that work effectively can be manufactured.The proposed metal matrix composite (MMC) perforated fins in this study significantly enhances the heat transfer rate.

REFERENCES

1. M.R. Shaeri, B. Richard, R. Bonner, Heat transfer and pressure drop in laterally perforated-finned heat sinks across different flow regimes, *Int. J. Heat Mass Transf.* 87 (2017) 220–227.
2. S. Chingulpitak, H.S. Ahn, L.G. Asirvatham, S. Wongwises, Fluid flow and heat transfer characteristics of heat sinks with laterally perforated plate fins, *Int. J. Heat Mass Transf.* 138 (2019) 293–303.

3. D.K. Kim, Thermal optimization of branched-fin heat sinks subject to a parallel flow, *Int. J. Heat Mass Transf.* 77 (2014) 278–287.
4. H.E. Ahmed, Optimization of thermal design of ribbed flat-plate fin heat sink, *Appl. Therm. Eng.* 102 (2016) 1422–1432.
5. Cola, B.A, "Carbon nanotubes as high performance thermal interface materials", *Electronics cooling* (2010) issue: April 2010.
6. Gwinn, J.P. and Webb, R.L. "Performance and testing of thermal interface materials", *Microelectronics Journal* 34 (2003) 215–222.
7. Kaczmar, J.W.Pietrzak, K. and Wlosinski, W. "The production and application of metal matrix composite materials", *Journal of Materials Processing Technology*106 (2000) 58–67.
8. Shaeri, M. R., & Bonner, R. (2017).Laminar forced convection heat transfer from laterally perforated-finned heat sinks.*Applied Thermal Engineering*, 116, 406–418.
9. M.R. Shaeri, M. Yaghoubi, Numerical analysis of turbulent convection heat transfer from an array of perforated fins, *Int. J. Heat Fluid Flow* 30 (2009) 218–228.
10. W. Al-Sallami,A. Al-Damook, H.M.Thompson, A numerical investigation of the thermal-hydraulic characteristics of perforated plate fin heat sinks, *Int. J. Therm. Sci.*121 (2017) 266–277.
11. M.R. Shaeri, M. Yaghoubi, K. Jafarpur, Heat transfer analysis of lateral perforated fin heat sinks, *Appl. Energy* 86 (2009) 2019–2029.
12. K.H. Dhanawade, V.K. Sunnapwar, H.S. Dhanawade, Thermal analysis of square and circular perforated fin arrays by forced convection, *Int. J. Curr. Eng. Technol.* 2 (2) (2014) 109–114.
13. K.H. Dhanawade, V.K. Sunnapwar, H.S. Dhanawade, Optimization of design parameters for lateral circular perforated fin arrays under forced convection, *Heat Transf. Asian Res.* 45 (2016) 30–45.
14. S.J. Kim, D.-K. Kim, H.H. Oh, Comparison of fluid flow and thermal characteristics of plate-fin and pin-fin heat sinks subject to a parallel flow, *Heat Transf. Eng.* 29 (2) (2008) 169–177.
15. H.Y. Li, S.M. Chao, Measurement of performance of plate-fin heat sinks with cross flow cooling, *Int. J. Heat Mass Transf.* 52 (2009) 2949–2955.
16. C.J. Shih, G.C. Liu, Optimal design methodology of plate-fin heat sink for electronic cooling system using entropy generation strategy, *IEEE Trans. Compon. Packag. Manuf. Technol.* 27 (3) (2004) 551–569.
17. H.H. Wu, Y. Y. Hsiao, H.S. Huang, P.H. Tang, S.L. Chen, A practical plate-fin heat sink model, *Appl. Therm. Eng.* 31 (2011) 984–992.
18. M.R. Shaeri, M. Yaghoubi, Thermal enhancement from heat sinks by using perforated fins, *Energy Convers. Manag.* 50 (2009) 1264–1270.
19. M.R. Shaeri, T.-C. Jen, Turbulent heat transfer analysis of a three-dimensional array of perforated fins due to changes in perforation sizes, *Numer. Heat Transfer Part A* 61 (2012) 807–822.
20. A. Subasi, B. Sahin, I. Kaymaz, Multi-objective optimization of a honeycomb heat sink using Response Surface Method, *Int. J. Heat Mass Transf.* 101 (2016) 295–302.
21. Ismail MF, Reza MO, Zobaer MA, Ali M. Numerical investigation of turbulent heat convection from solid and longitudinally perforated rectangular fins. *ProcediaEng* 2013; 56:454e97.
22. Gaofeng Lu, XiaoqiangZhai "Analysis on heat transfer and pressure drop of a microchannel heat sink with dimples and vortex generators" *International Journal of Thermal Sciences* 145 (2019) 105986.
23. Daxiang Deng, Guang Pi, Weixum Zhang, Peng Wang, and Ting Fu, "Numerical Study of Double-Layered Microchannel Heat Sinks with Different Cross-Sectional Shapes".*Entropy* 2019, 21(1), 16; <https://doi.org/10.3390/e21010016>
24. Soheil Soleimanikutanaei, EsmailGhasemisahebi, Cheng-Xian Lin, "Numerical study of heat transfer enhancement using transverse microchannels in a heat sink" *International Journal of Thermal Sciences* 125 (2018) 89–100.
25. Nor Azwadi Che Sidik, Muhammad Noor AfiqWitri Muhamad, Wan MohdArif Aziz Japar, Zainudin A. Rasid, "An overview of passive techniques for heat transfer augmentation in microchannel heat sink" *International Communications in Heat and Mass Transfer* 88 (2017) 74–83.
26. Xiaoming Huang, Wei Yang, Tingzhen Ming, Wenqing Shen, Xiangfei Yu, "Heat transfer enhancement on a microchannel heat sink with impinging jets and dimples" *International Journal of Heat and Mass Transfer* 112 (2017) 113–124.
27. Sajjad Baraty Beni, Alireza Bahrami, Mohammad Reza Salimpour, "Design of novel geometries for microchannel heat sinks used for cooling diode lasers" *International Journal of Heat and Mass Transfer* 112 (2017) 689–698

28. Sainan Lu, KambizVafai, "A comparative analysis of innovative microchannel heat sinks for electronics cooling International Communications in Heat and Mass Transfer 76 (2016) 271–284.
29. Narender Panwar, Amit Chauhan, "Fabrication methods of particulate reinforced Aluminium metal matrix composite - A review". ICMPC 2017.
30. Bhaskar Chandra Kandpal, Jatinder Kumar, Hari Singh, "Manufacturing and technological challenges in Stir casting of metal matrix composites – A Review". PMME 2016.
31. Ch.HimaGireesh, K.G.Durga Prasad, K.Ramji, P.V.Vinay, "Mechanical Characterization of Aluminium Metal Matrix Composite Reinforced with Aloe vera powder". ICMPC 2017.

AUTHORS PROFILE



E. Nirmala devi, working as an Associate Professor in the Department of Mechanical Engineering, Godavari Institute of Engineering and Technology(Autonomous), Rajahmundry, India.



T. Rajesh, pursuing M. Tech in thermal engineering in the Department of Mechanical Engineering, Godavari Institute of Engineering and technology(Autonomous), Rajahmundry, India.